This article appeared in Applied Physics Letters **120**(3), 033103 (2022) and may be found at https://doi.org/10.1063/5.0080133

The formation of a one-dimensional van der Waals selenium crystal from the three-dimensional amorphous phase: a spectroscopic signature of van der Waals bonding

M. Krbal*
Center of Materials and Nanotechnologies (CEMNAT), Faculty of Chemical Technology, University of Pardubice, 530 02 Pardubice, Czech Republic

A.V. Kolobov*
Department of Physical Electronics, Institute of Physics, Herzen State Pedagogical University of Russia, St. Petersburg 191186, Russia and Device Technology Research Institute, National Institute of Advanced Industrial Science and Technology, Tsukuba 305-8568 Ibaraki, Japan

P. Fons
Faculty of Science and Technology, Department of Electronics and Electrical Engineering, Keio University, Yokohama, Kanagawa 223- 8522, Japan and Device Technology Research Institute, National Institute of Advanced Industrial Science and Technology, Tsukuba 305-8568 Ibaraki, Japan

Y. Saito
Device Technology Research Institute, National Institute of Advanced Industrial Science and Technology, Tsukuba 305-8568 Ibaraki, Japan

G. Belev and S. Kasap
Electrical and Computer Engineering, University of Saskatchewan, 57 Campus Drive, Saskatoon, SK, S7N5A9, Canada

(Dated: January 6, 2022)

Trigonal selenium is a prototypical one-dimensional (1D) van der Waals (vdW) solid, where covalently bonded helical chains are held together by weaker vdW forces. In this work, we have studied structural transformation from a three-dimensional amorphous phase of non-interacting Se chains into a 1D vdW crystal using X-ray absorption spectroscopy. The crystallization process and establishment of vdW interaction is accompanied by elongation and weakening of covalent Se-Se bonds. We have found a unique signature in the X-ray absorption near-edge structure (XANES) spectrum that is associated with vdW bonds and can be used to identify the formation of the latter. We believe that a similar approach can be used to study other 1D vdW solids, such as transition-metal trichalcogenides, and particularly stress the usefulness of x-ray absorption spectroscopy to identify vdW bonds.

When it comes to one-dimensional (1D) van der Waals (vdW) crystals, the prototypical examples are trigonal chalcogens such as Selenium and Tellurium. These crystals are made from helical chains consisting of two-fold coordinated covalently bonded chalcogen atoms. The chains are held together by much weaker vdW forces. The ability to form vdW bonds is thanks to the presence of pairs of non-bonding p-electrons (so-called lone-pair electrons), which are easily polarisable leading to the appearance of dispersion forces. The interest in selenium / tellurium in this context is further underscored by the fact that most two-dimensional (2D) vdW solids such as transition-metal dichalcogenides with the generic formula MX_2 (M = Mo, W, V, etc., X = S, Se, Te) [1], classic topological insulators (Sb_2Te_3, Sb_2Se_3, Bi_2Te_3) [2] as well as $A^{III}B^{VI}$ layered materials (e.g. InSe [3]) all contain chalcogen species and vdW gaps are formed between atomic planes of the latter. Recently, a different class of materials, with 1D motifs in their crystalline structures, has been attracting a lot of attention, namely transition metal trichalcogenides [4], which are a prominent group of quasi-1D materials that consist of strongly bonded one-dimensional chains weakly bonded to neighboring chains. The fact that various classes of vdW solids contain chalcogen atoms and that the vdW gaps are actually formed between those chalcogen atoms makes the study of elemental vdW chalcogenides of special interest.

Certain understanding of the physics and chemistry of bonding comes from the consideration of electron occupancy in chalcogens. Chalcogens possess two s- and four p-electrons. From the latter, two are isolated on p_x and p_y orbitals and serve to form covalent bonds, while the remaining two form a lone-pair. The bonding and lone-pair electrons can be readily visualised from ab-initio simulations as charge-density difference (CDD) clouds, which represent the difference between the electron density in

the material studied and non-interacting atoms. Thus the CDD clouds between pairs of atoms is a signature of a covalent bond and increased electron density represented by two clouds correspond to lone-pair electrons (Supplementary information, Fig. 1S).

It is worth noting that lone-pair electrons, on the one hand, are not involved in the formation of covalent bonds but, on the other hand, they occupy the highest occupied orbitals, i.e. they form the top of the valence band and consequently determine the electronic structure (and properties) of the material [5]. For this reason the term lone-pair semiconductors was proposed to describe such materials. As a consequence, when individual chains move with respect to each other due to the weakness of vdW bonds in the crystalline phase or their absence (or significantly weaker manifestation) in the amorphous phase, the interaction of lone-pair electrons changes and, accordingly, changes the electronic structure.

A prototypical example of such a process is reversible photostructural changes, where the absorption edge shifts to lower energies upon exposure to (above) band-gap light, whereas the initial absorption is restored upon annealing [6]. In-situ EXAFS [7] and ESR [8, 9] measurements demonstrated that this change is due to the formation (and rupture) of interchain bonds due to involvement of lone-pair electrons. Another interesting feature of amorphous selenium (a-Se) is its ability to crystallize under photo-exposure. While the thermal effect of light may play a certain role, optical excitation is crucial to this process. In particular, it was found that the direction of the *c*-axis of the crystalline phase strongly correlates with the polarisation of the acting light [10–12]. Moreover, when an a-Se film was exposed to a simultaneous action of red (λ = 633 nm) and green (λ = 514 nm) laser beams, the crystallization rate was an order of magnitude different for parallel and perpendicular orientations of the polarisation planes of the two laser beams [13]. At the same time, exposure of the crystalline film - at temperatures as low as 77 K - resulted in photomelting of selenium [14]. These results demonstrate the possibility to use electronic excitation to modify the structure through establishing, or breaking, vdW interaction between the chains thus opening an interesting opportunity in materials design.

In this work we have studied the process of the formation of the ordered crystalline phase by means of solid-state crystallization of the amorphous phase. Samples were prepared by thermal evaporation of 1 μm of selenium onto both sides of a Kapton film kept at room temperature. The as-deposited samples were amorphous as was confirmed by X-ray diffraction measurements. To obtain crystalline films, the as-deposited samples were annealed in vacuum at 100 °C for three hours.

X-ray absorption measurements were performed at beamline BL01B1 at SPring-8 in transmission mode in a temperature range from 10 K to 403 K. The Kapton foil with Se was cut into pieces and stacked to insure an absorption jump of ca. 1. Analysis was performed using the Demeter package [15]. In the fitting process the coordination number of crystalline selenium (c-Se) was set to be CN = 2.0.

The amorphous phase was generated by means of *ab-initio* molecular dynamics via a melt quench process using the plane-wave density-functional theory program VASP 6 [16]. To create the amorphous phase, a unit cell containing 192 Se atoms was constructed with a density $\rho = 4.03\ \mathrm{gm\,cm^{-3}}$ (5% lower than the crystalline phase). The structure was then randomized at 1000 K for 10 ps. Following the randomization, the structure was quenched from 1000 to 500 K over a period of 5 ps. The resulting quenched structure was then equilibrated at 500 K for 15 ps and then finally cooled to 0 K over a period of 15 ps. The value for the plane wave cutoff was 211 eV following the recommendations of the VASP authors in the projector augmented wave pseudopotential file. The gamma point was used for integrations in the Brillouin zone.

The theoretical XANES spectra were calculated using the ab-initio real-space full multiple-scattering code FEFF9 [17] via relaxed prototypical models of amorphous and annealed GeTe-based alloys. FEFF9 is a fully relativistic, all-electron Green function code that utilizes a Barth-Hedin formulation for the exchange-correlation part of the potential and the Hedin-Lundqvist self-energy correction. In our FEFF calculations, the cluster radius was set to 9 Å around the central atom, which corresponds to about 100 atoms in the model. XANES spectra were calculated for each of the 192 atoms in the final 0K unit cell.

Figure 1 shows raw EXAFS oscillations (A) and Fourier transformed spectra (B) for the amorphous and crystalline films. One can see that the EXAFS quality is very high with practically noiseless data till 20 $\mathrm{Å^{-1}}$. In the Fourier transformed spectrum for c-Se the main (first-nearest neighbor) peak is followed by several higher-shell peaks, which is characteristic of a solid with long-range order. The peak notations are illustrated in the inset to panel (B). Namely, Se1 is the first-nearest neighbor within the same chain, Se3 corresponds to the distance between two atoms bonded to a central atom in the same chain. Both Se1 and Se3 are different int*ra*chain distances. The peak Se2 corresponds to the distance between two neighboring chain (the int*er*chain distance).

Interestingly, a higher shell (Se3) is also clearly visible in a-Se. We should note here that the peak corresponding to Se3 is also clearly observed in the pair-distribution function obtained from the melt-quenched Se model (Suppl. Fig. S1). The result suggests that the valence angles (between *p*-orbitals) subtended at Se atoms are rather rigid despite the overall lability of the structure.

One can further see that the Se1 peak for a-Se is lo-

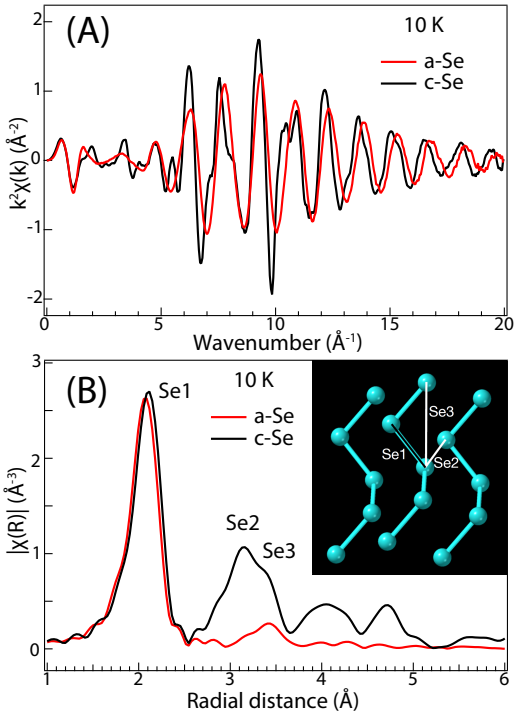

FIG. 1: Raw EXAFS oscillations (A) and Fourier transformed spectra (B) for a- and c-Se measured at 10 K. The inset illustrates the peak notations.

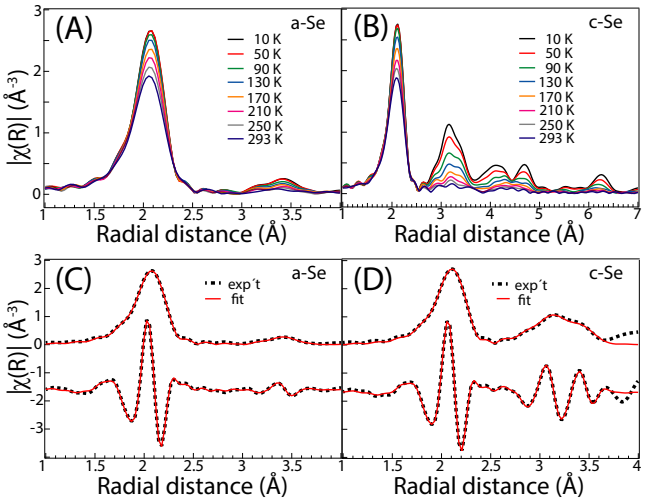

FIG. 2: Temperature evolution of Fourier transformed spectra for a- (A) and c-Se (B). Lower panels demonstrate the quality of the 10 K fits for a- (C) and c-Se (D). The fits are shown for the amplitude (upper curve) and real part (lower curve) of the Fourier transformed spectra.

cated at a shorter distance compared to the crystalline phase, in agreement with earlier observations [7]. This result is highly unusual (typically, due to bond anharmonicity, bonds are longer in the amorphous phase) and suggests that chain ordering upon crystallization is accompanied by a change in bonding nature.

A similar result, Ge-Te bond shortening, in the amorphous phase, was also observed in a $Ge_2Sb_2Te_5$ (GST) phase change alloy [18], where it was attributed to a change in bonding from purely covalent in the amorphous phase to resonant [19, 20] (also recently referred to as metavalent [21]) in the crystalline phase. Since both Se and phase-change alloys are characterised by the presence of primary and secondary bonds (covalent intrachain bonds vs. vdW interchain bonds in Se and shorter vs. longer bonds in GST) one could argue that bond elongation in the crystalline phase is associated with the formation of weaker secondary bonds.

Figure 2 (panels A and B) shows the variation of the Fourier transformed spectra for the amorphous and crystalline phases with temperature, namely the peak intensity decreases as the temperature is increased. The lower panels (C) and (D) demonstrate the high quality of the fits in both cases. Table I summarises the fitting results. The slightly smaller coordination number for the first-nearest neighbors in a-Se suggests the presence of short chains, and consequently chain ends. This result is in agreement with photo-ESR measurements [8, 9]. The temperature variation of the obtained structural parameters is shown in Suppl. Fig. S2.

TABLE I: Coordination numbers (CN), bond lengths (BL) and mean-square relative displacement (MSRD) of as-deposited and crystallized Se

Bonds	CN	BL/Å	MSRD/Å^2
aSe1	1.88± 0.05	2.35 ± 0.01	0.0025 ± 0.0001
aSe3	0.85 ± 0.28	3.69 ± 0.02	0.0048 ± 0.002
cSe1	2.0	2.38 ± 0.01	0.0026 ± 0.0001
cSe2	3.92± 0.84	3.40 ± 0.01	0.0065 ± 0.0002
cSe3	1.08 ± 0.50	3.73 ± 0.01	0.0024 ± 0.0003

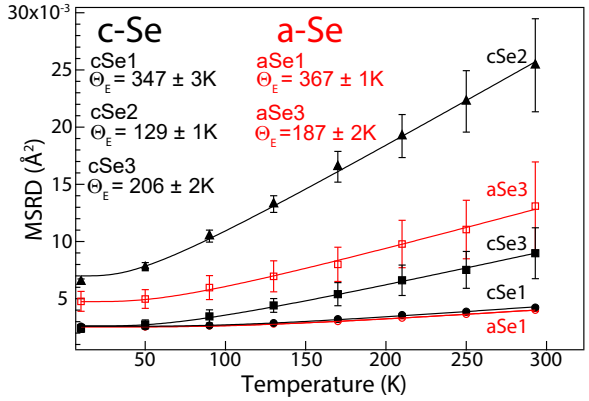

FIG. 3: Temperature dependences of MSRD for various peaks for a- and c-Se. The fitting results (the Einstein temperature) are shown as legend.

In Fig. 3 we show the temperature dependence of the mean-square relative displacement (MSRD), a disor-

der parameter somewhat similar to Debye-Waller (DW) factor. The critical difference between the two is that the DW factor characterises deviation of an (individual) atom from its equilibrium position, while MSRD is a measure of disorder in *interatomic distances*. The extent to which MSRD increases with temperature as well as its absolute value are determined by the bond strength usually represented by an Einstein temperature Θ_E that is related to MSRD, σ, through the following equation:

$$\sigma^2 = \frac{\hbar^2}{2\mu k_B \Theta_E} \coth \frac{\Theta_E}{2T} + \sigma_0^2$$

Here, μ is the reduced mass, k_B is Boltzmanns constant, and σ_0 is the static disorder. A larger Einstein temperature indicates a stronger bond. The fitting results are also shown in Fig. 3.

One can see that Θ_E(Se1) for c-Se is a little smaller than that for a-Se, which indicates stronger covalent bonds in the amorphous phase. This result is in agreement with the shorter bonds in the amorphous phase and also with the higher frequency of Raman scattering observed in a-Se with respect to its crystalline counterpart [22]. At the same time, the Θ_E(Se3) is notably larger in the crystalline phase. Since the Se3 distance characterises the rigidity of covalent angles within a chain, the result is readily understood: it is easier to distort an angle in an isolated chain than that in a structure consisting of interacting chains.

Of special interest is the significantly smaller Θ_E(Se2) value. Typically, the shorter the distance, the stronger the interaction. The fact that Θ_E(Se2) is smaller than Θ_E(Se3) is unambiguous evidence of a difference in chemical bonding: while the Se1 and Se3 are determined by covalent bonds, the Se2 has a different chemical nature. Namely, the interaction between chains is due to significantly weaker vdW forces.

Figure 4 shows the evolution of the Se1 peak during the crystallization process, one can see that the Se-Se first nearest distance continuously increases with temperature but no further details of the process can be deducted from EXAFS analysis.

We now turn to the most exciting finding of this work. In Fig. 5 (panel A) the X-ray absorption near-edge structure (XANES) spectra of the amorphous and crystalline phases are compared and panel C shows the evolution of XANES (a zoomed-in image) upon the amorphous-to-crystal transition. Several aspects of result shown on Fig. 5(C) should be stressed. One is the presence of so called isosbestic points. In spectroscopy, an isosbestic point is a specific wavelength, wavenumber or frequency at which the total absorbance of a sample does not change during a chemical reaction or a physical change of the sample (the word derives from Greek words "iso" (equal) and "sbestos" (extinguishable)). In chemical kinetics, isosbestic points are used as reference points in the study of reaction rates, as the absorbance at those wavelengths

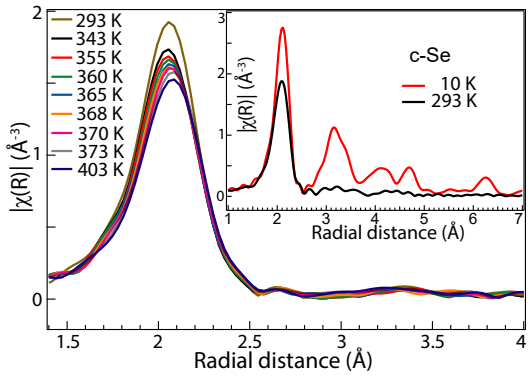

FIG. 4: Thermal evolution of EXAFS during the crystallization process in a temperature range from 343 K to 403 K. The room temperature spectrum is also shown for comparison. The inset compares EXAFS spectra for c-Se at 10 K and at room temperature. One can see that the room temperature spectrum is dominated by the first shell (and looks similar to the amorphous spectrum), higher shells are essentially at a noise level.

remains constant throughout the whole reaction. The presence of isosbestic points provides proof for a direct conversion of one phase to another without intermediary or side products.

One can see that the peak "C" located (at 12667 eV) to the left of the isosbestic point "1" and corresponding to covalent bonding that prevails in the amorphous phase decreases, while the peak "vdW" located at higher energies appears and grows during the formation of a 1D vdW structure from a three-dimensional amorphous phase. The strength of the "vdW" peak is thus a measure of the extent to which vdW forces link together individual Se chains. The presence of the "vdW" peak in the crystalline phase has also been confirmed by ab-initio simulations using the FEFF code applied to the melt-quenched amorphous structure obtained from ab-initio molecular dynamics simulations (Fig. 5(B)). The crystalline and amorphous structures used for FEFF simulations are shown in supplementary information (Fig. S3).

Of special interest is the fact that, while EXAFS oscillations change with temperature (as evidenced by the decrease of the intensity of the first shell and nearly disappearance of higher shells at higher temperatures and also illustrated by Fig. S4 where the raw EXAFS oscillations for a-Se and c-Se at 10 K and room temperature are shown), the shape of XANES spectra, essentially does not depend on temperature as is illustrated by the inset to Fig. 5(C), where XANES spectra for a-Se and c-Se at 10 K and at room temperature are compared. One can see that the thermal effect on XANES is negligible. As a consequence, the appearance and the intensity of the "vdW" peak in XANES spectrum can be a reliable signature of the presence of vdW bonds in a system of

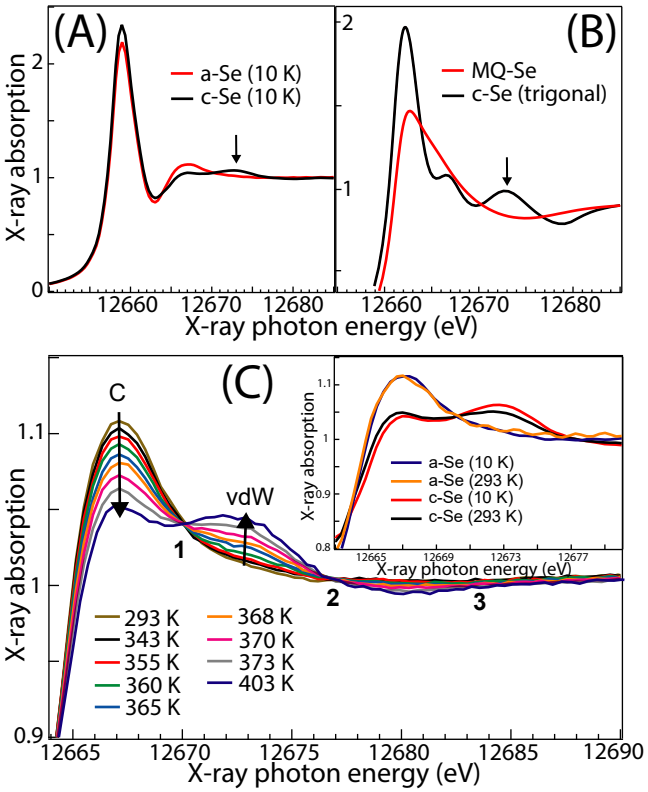

FIG. 5: Experimental (A) and simulated (B) XANES spectra for a- and c-Se. The peak, associated with vdW bonds is shown by arrows. Panel (C): a zoomed-in image of the evolution of XANES upon crystallization of Se. As the crystallization proceeds, the "covalent" peak "C" decreases, while the vdW peak grows. The inset shows the XANES spectra of a- and c-Se at 10 K and room temperature: the spectra are essentially temperature independent.

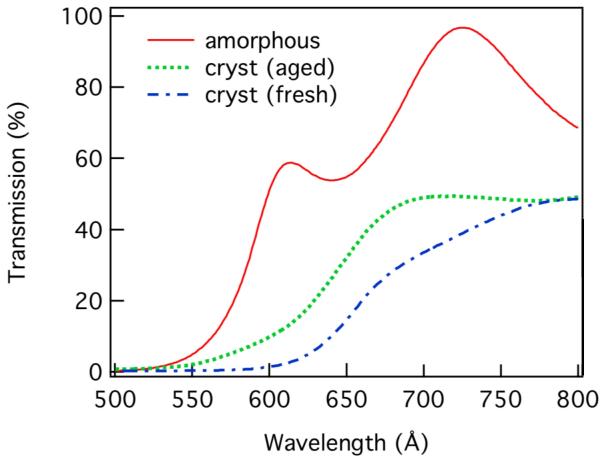

FIG. 6: Absorption spectra of an as-deposited a-Se film and two identical films crystallized for 6 hours at 70 °C: one was crystallized immediately from the as-deposited state and the other one was kept in the dark (aged) at 30 °C for 3 months prior to annealing.

Se chains.

Finally, we would like to note that the presence of shorter chains in a-Se as discussed above helps establishing the 1D vdW crystal. If the amorphous phase is kept for a long time, (some of the) chain ends may interact with neighboring chains and form valence alternation pairs [23], cross-linking the structure. Once the amorphous phase has been cross-linked (similar to entangled spaghettis), it becomes more difficult to form the 1D crystalline phase. We illustrate this statement by Fig. 6, where the optical transmission spectra of an as-deposited a-Se film is shown in comparison with the annealed (70 °C, 6 hours) two pieces of the same film, of which one was annealed immediately after deposition, and the other has been kept in the darkness at room temperature for 3 months prior to crystallization. Since the band gap of c-Se is smaller that that of a-Se, the observed shift of the absorption edge to longer wavelength is a measure of the degree of crystallization. One can clearly see a significantly stronger effect of annealing of the freshly deposited film with a larger concentration of shorter chains.

In conclusion, we have performed an x-ray absorption study of the formation of a 1D vdW crystal - selenium - through solid-state crystallization from a three-dimensional amorphous phase. Our results demonstrate an unusual change in the bond length and bond strength upon crystallization, namely bond elongation and weakening upon crystallization, which is an unambiguous indication of the different bonding nature in the amorphous and crystalline phases. We have discovered a characteristic fingerprint in XANES spectrum of Se that can be used to identify the presence of vdW bonding.

See the supplementary material for the information regarding the structural details of the amorphous and crystalline Se and the temperature evolution of the first nearest neighbor coordination number and Se-Se bond length variation.

This work was supported by the Russian Foundation for Basic Research (RFBR)-Japan Society for the Promotion of Science (JSPS) Bilateral Joint Research Projects (Russia-Japan) (Grant Nos. RFBR 20-52-50012 and JPJSBP120204815). MK acknowledges financial support from the Czech Science Foundation 19-17997S, the Ministry of Education, Youth and Sports (LM2018103).

The data that support the findings of this study are available from the corresponding author upon reasonable request.

* Authors to whom correspondence should be addressed: Milos.Krbal@upce.cz, akolobov@herzen.spb.ru

[1] A. Kolobov and J. Tominaga, *Two-Dimensional Transition-Metal Dichalcogenides* (Springer International Publishing, 2016).

[2] H. Zhang, C.-X. Liu, X.-L. Qi, X. Dai, Z. Fang, and S.-C. Zhang, Nature Phys. **5**, 438 (2009).

[3] D. A. Bandurin, A. V. Tyurnina, G. L. Yu, A. Mishchenko, V. Zólyomi, S. V. Morozov, R. K. Kumar, R. V. Gorbachev, Z. R. Kudrynskyi, S. Pezzini, et al., Nature Nanotech. **12**, 223 (2017).

[4] A. Patra and C. Rout, RSC Adv. **10**, 36413 (2020).

[5] M. Kastner, Phys. Rev. Lett. **28**, 355 (1972).

[6] K. Tanaka and A. Odajima, Solid State Commun. **43**, 961 (1982).

[7] A. Kolobov, H. Oyanagi, K. Tanaka, and K. Tanaka, Phys. Rev. B **55**, 726 (1997).

[8] A. V. Kolobov, M. Kondo, H. Oyanagi, R. Durny, A. Matsuda, and K. Tanaka, Phys. Rev. B **56**, 485 (1997).

[9] A. V. Kolobov, M. Kondo, H. Oyanagi, A. Matsuda, and K. Tanaka, Phys. Rev. B **58**, 12004 (1998).

[10] V. Tikhomirov, P. Hertogen, C. Glorieux, and G. Adriaenssens, Phys. Stat. Sol. (a) **162**, R1 (1997).

[11] V. Poborchii, A. Kolobov, and K. Tanaka, Appl. Phys. Lett. **72**, 1167 (1998).

[12] V. Lyubin, M. Klebanov, and M. Mitkova, Appl. Surf. Sci. **154**, 135 (2000).

[13] A. Roy, A. Kolobov, and K. Tanaka, J. Appl. Phys. **83**, 4951 (1998).

[14] V. V. Poborchii, A. V. Kolobov, and K. Tanaka, Appl. Phys. Lett. **74**, 215 (1999).

[15] B. Ravel and M. Newville, J. Synchrotron Rad. **12**, 537 (2005).

[16] G. Kresse and J. Hafner, Phys. Rev. B **49**, 14251 (1994).

[17] A. Ankudinov and J. Rehr, Phys. Rev. B **62**, 2437 (2000).

[18] A. Kolobov, P. Fons, A. Frenkel, A. Ankudinov, J. Tominaga, and T. Uruga, Nature Mater. **3**, 703 (2004).

[19] G. Lucovsky and R. White, Phys. Rev. B **8**, 660 (1973).

[20] K. Shportko, S. Kremers, M. Woda, D. Lencer, J. Robertson, and M. Wuttig, Nature Mater. **7**, 653 (2008).

[21] M. Wuttig, V. L. Deringer, X. Gonze, C. Bichara, and J.-Y. Raty, Advanced Materials **30**, 1803777 (2018).

[22] A. Mooradian and G. B. Wright, in *Proceedings of the International Symposium, Physics of Selenium and Tellurium*, edited by W. C. Cooper (Pergamon Press, 1969), pp. 269–276.

[23] M. Kastner, D. Adler, and H. Fritzsche, Phys. Rev. Lett. **37**, 1504 (1976).